

Supporting information

Synthesis of a stable iron(III)-organic framework for visible light induced simultaneous photocatalytic reduction of Cr(VI) and degradation of organic dyes in water

A-Di Xie,^{a, #} Ming-Gai Hu,^{a, #} Yu-Hui Luo,^{a, *} Xiang-Gui Zhu,^a Zhi-Hui Wang,^b Wu-Yue Geng,^a Hao Zhang,^a Dong-En Zhang,^{a, *} and Hong Zhang^{b, *}

^a School of Environmental and Chemical Engineering, Jiangsu Ocean University, Lianyungang 222000, P. R. China

^b Institute of Polyoxometalate Chemistry, Department of Chemistry, Northeast Normal University, Changchun, Jilin 130024, P. R. China

[#] These two authors contributed equally.

* Corresponding authors. E-mail: luoyh@jou.edu.cn (Yu-Hui Luo),
2007000040@jou.edu.cn (Dong-En Zhang),
zhangh@nenu.edu.cn (Hong Zhang).

Materials and Measurements

All reagents and solvents were purchased from commercial sources and used without further purification. Powder X-ray diffraction (PXRD) patterns were collected on a PANalytical X'Pert Powder X-ray diffractometer with graphite monochromatized Cu K α radiation ($\lambda = 0.15418$ nm) and 2θ ranging from 3 to 50 $^\circ$ with an increment of 0.02 $^\circ$ and a scanning rate of 10 $^\circ$ /min. The FT-IR spectrum was measured in KBr pellets in the range 4000-400 cm^{-1} on a Thermo Scientific spectrometer. The UV-Vis absorption was measured with a PERSEE UV-Vis-NIR spectrophotometer. Mott-Schottky measurements and short circuit photocurrent response was performed on a CHI660E electrochemical workstation from Shanghai Chenhua Instrument Co., Ltd. Inductively coupled plasma optical emission spectrometry (ICP-OES) were performed on an Optima 8000 from PerkinElmer. X-ray photoelectron spectroscopy (XPS) were carried out on a NexsaTM X instrument from Thermo ScientificTM. The Brunauer-Emmett-Teller (BET) surface areas was determined by BSD-PS1 instrument from BeiShiDe Instrument technology (Beijing) Co. Ltd.

X-ray crystallography

Crystallographic diffraction data for **JOU-22** were recorded on an Oxford Gemini S Ultra diffractometer with graphite monochromatized Cu-K α radiation ($\lambda = 1.5418$ Å) at room temperature. the structure was solved by Direct Method of SHELXT-2016 and refined by full-matrix least-squares techniques by using the SHELXL-2016 program.¹ All nonhydrogen atoms were refined with anisotropic temperature parameters. All hydrogen atoms were placed in geometrically idealized position as a riding mode. The solvent molecules in the crystal are highly disordered and are removed by using the SQUEEZE routine of PLATON.² ISOR command was used to restrict O1W and O2 for ADP alert. The crystallographic data for **JOU-22** were summarized in Table S1, and the selected bond lengths and angles are listed in Table S2. CCDC number for **JOU-22** is 2026455.

Table S1. Crystal data and structure refinements for **JOU-22**.

	JOU-22
Empirical formula	C ₈ H ₆ O ₆ Fe
Formula weight	253.98
Temperature / K	100.00(10)
Wavelength / Å	1.5418
Crystal system	tetragonal
Space group	<i>I</i> 4 ₁ 22
<i>a</i> / Å	15.1494(10)
<i>b</i> / Å	15.1494(10)
<i>c</i> / Å	12.0558(2)
α / $^\circ$	90
β / $^\circ$	90

$\gamma / ^\circ$	90
Volume / \AA^3	2766.86(6)
Z	8
Reflns coll./unique	3320/
$F(000)$	1024.0
Density / g cm^{-3}	1.570
μ / mm^{-1}	9.050
R_{int}	0.0219
Goodness-of-fit on F^2	1.017
$R1, wR2 [I > 2\sigma(I)]^a$	0.0329, 0.1021
$R1, wR2$ (all data) ^a	0.0339, 0.1032

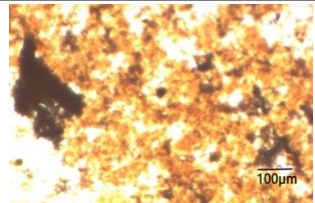
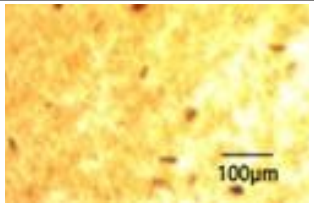
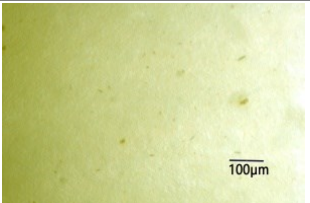
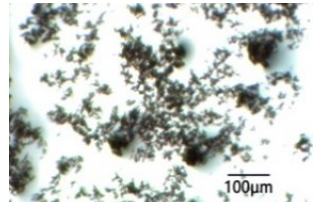
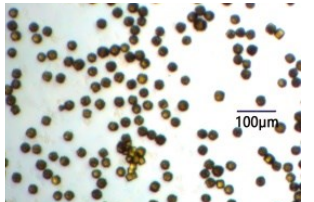
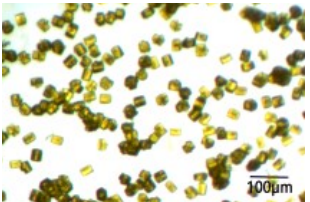
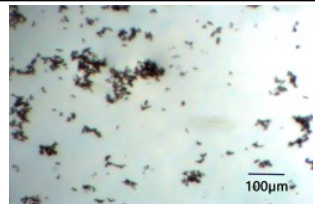
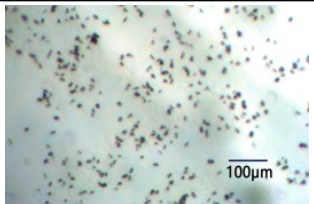
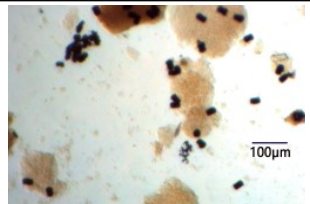
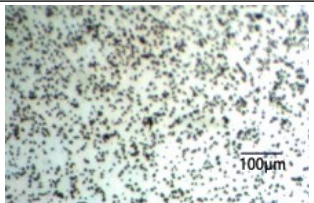

^a $R_1 = \sum ||F_o| - |F_c|| / \sum |F_o|$; $wR_2 = \sum [w(F_o^2 - F_c^2)^2] / \sum [w(F_o^2)^2]^{1/2}$.

Table S2. Selected bond lengths (\AA) and angles ($^\circ$) for **JOU-22**.^a

Fe1-O1 ^{#1}	1.954(2)	Fe1-O3 ^{#2}	2.022(2)
Fe1-O1	1.954(2)	Fe1-O2 ^{#1}	2.026(3)
Fe1-O3	2.022(2)	Fe1-O2 ^{#3}	2.026(3)
O3 ^{#2} -Fe1-O2 ^{#1}	90.57(12)	O1 ^{#1} -Fe1-O2 ^{#1}	89.37(10)
O1 ^{#1} -Fe1-O2 ^{#3}	169.60(11)	O1-Fe1-O3 ^{#2}	169.66(9)
O1-Fe1-O2 ^{#3}	89.37(10)	O3-Fe1-O2 ^{#1}	90.57(14)
O1 ^{#1} -Fe1-O1	100.91(14)	O3 ^{#2} -Fe1-O2 ^{#3}	90.62(13)
O1 ^{#1} -Fe1-O3	88.33(12)	O2 ^{#1} -Fe1-O2 ^{#3}	80.36(15)
O1-Fe1-O3	90.68(12)	O3-Fe1-O2 ^{#3}	90.62(13)
O1 ^{#1} -Fe1-O3 ^{#2}	90.68(12)	O3-Fe1-O3 ^{#2}	178.54(17)
O1-Fe1-O3 ^{#2}	88.32(12)		

^a Symmetry transformation used to generate equivalent atoms: #1, 0.5 - x, y, 0.25 + z; #2, 0.5 - x, 0.5 - y, 1.5 - z; #3, x, 0.5 - y, 1.25 - z.

Table S3. Optimization of synthesis conditions of **JOU-22** crystal.

Ln \ HF	0 mg	43 mg	64 mg
20 μL			
30 μL			
40 μL			
50 μL			

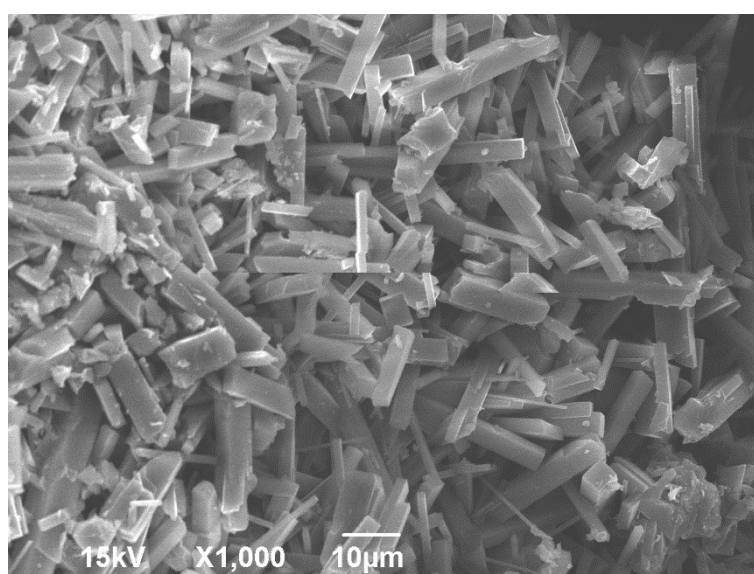


Fig. S1. SEM image of **JOU-22** powder. 30 μL HF was added during synthesis process.

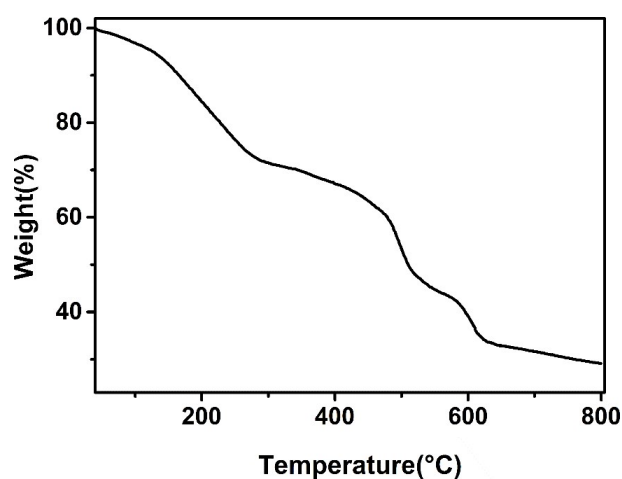


Fig. S2. TGA curve of JOU-22 crystals.

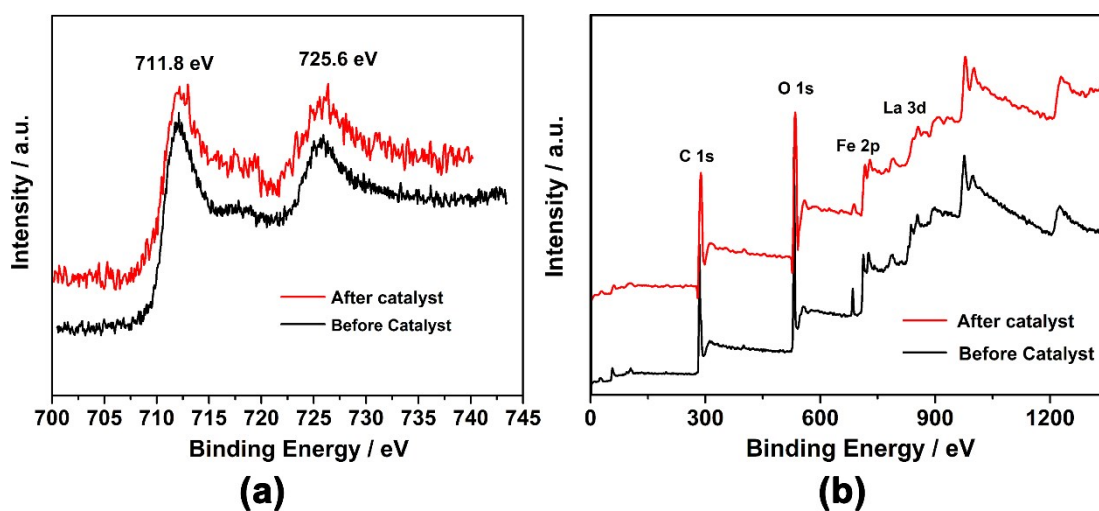


Fig. S3. (a) XPS high resolution spectra of iron in JOU-22 crystals before and after photocatalytic reaction. (b) XPS spectra of JOU-22 crystals before and after photocatalytic reaction.

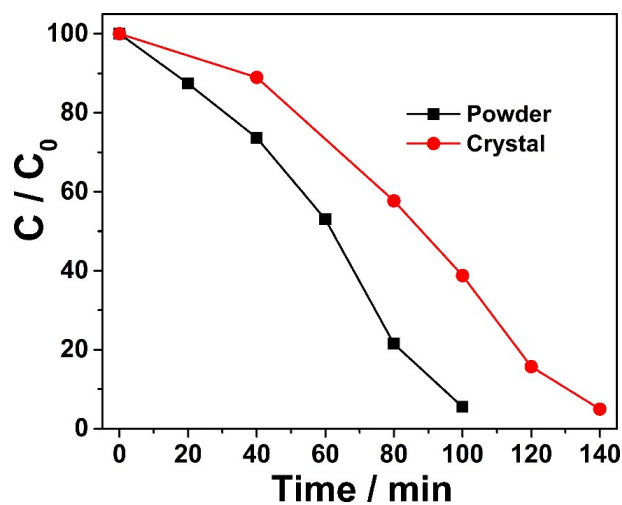


Fig. S4. Comparison of degradation efficiency of dichromate anions over JOU-22

crystals and powder.

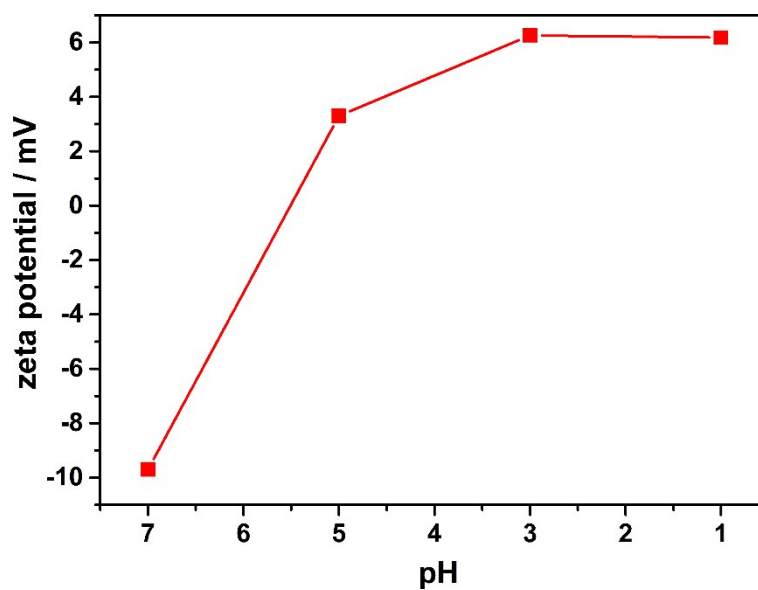


Fig. S5. As the proton concentration increases, the protonation of **JOU-22** makes its surface charge turn from negative to positive.

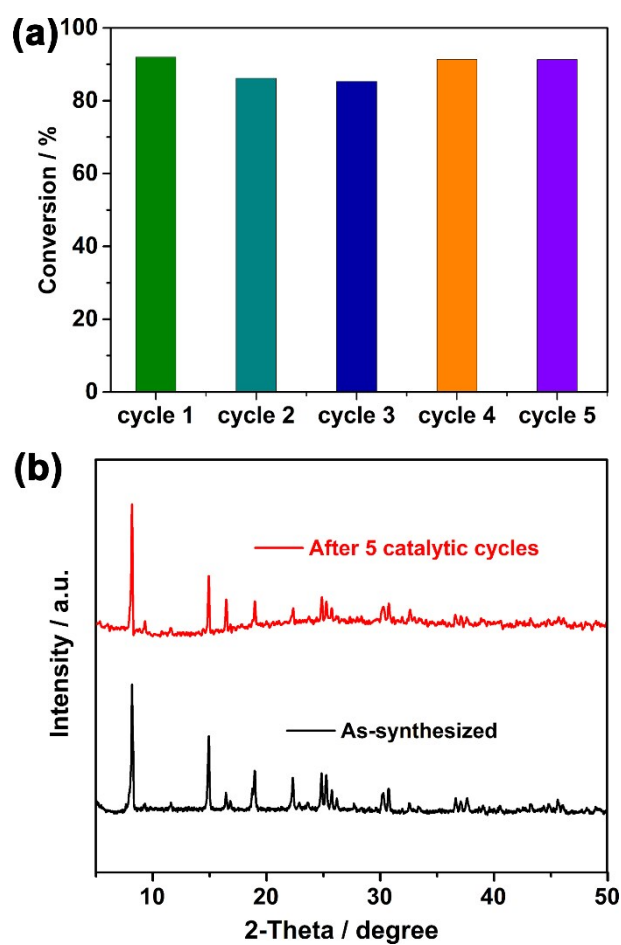


Fig. S6. (a) Photocatalytic activity of **JOU-22** almost unchanged over five reaction rounds. (b) PXRD pattern of **JOU-22** after five reaction rounds consists well with that

of as-synthesized samples.

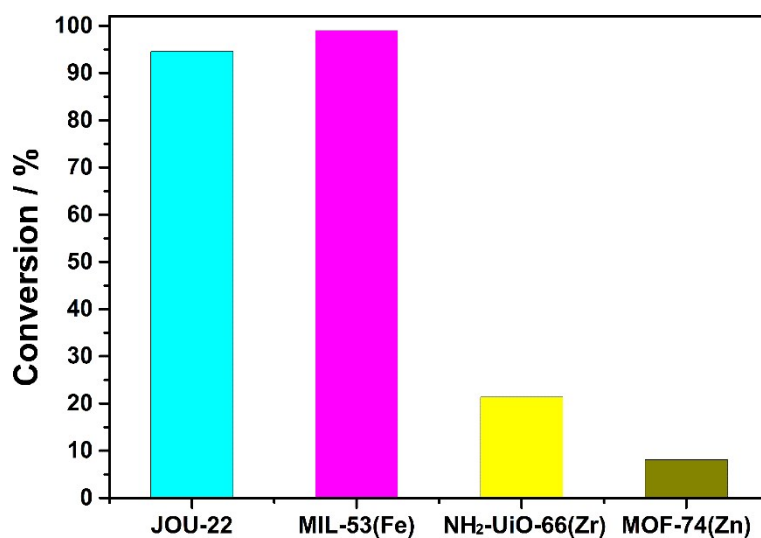


Fig. S7. Comparison of the Cr(IV) reduction rate over different MOF materials.

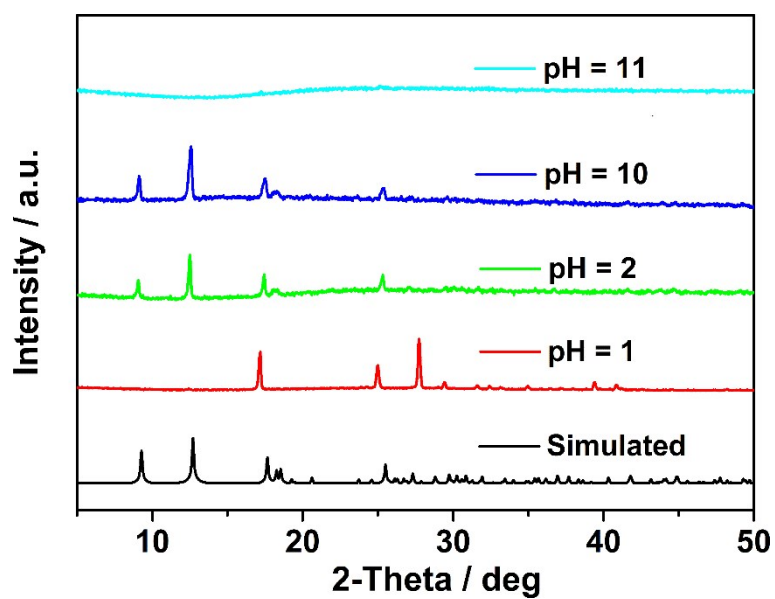


Fig. S8. MIL-53(Fe) can stable in aqueous solution with pH range from 2 - 10.

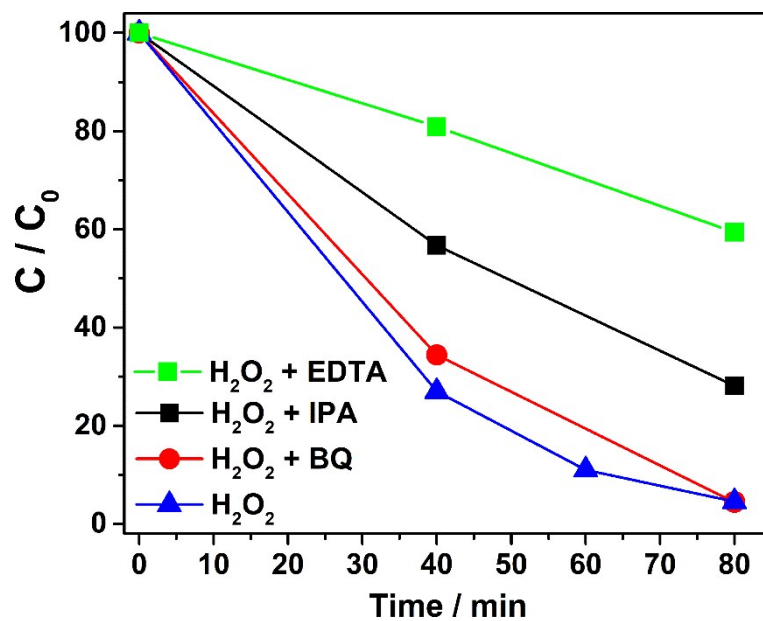


Fig. S9. Kinetics of photocatalytic MB degradation under different conditions.

References

1. (a) G. M. Sheldrick, *Acta Crystallogr. A*, 2008, **A64**, 112-122; (b) G. M. Sheldrick, *Acta Crystallogr. C*, 2015, **C71**, 3-8.
2. A. L. Spek, *J. Appl. Crystallogr*, 2003, **36**, 7-13.